1

2

3

Quantification and characterization of Ti-, Ce- and Ag-nanoparticles in global surface waters and precipitation

Agil Azimzada[1,2], Ibrahim Jreije[1], Madjid Hadioui[1], Phil Shaw[3], Jeffrey M. Farner[4], Kevin J. Wilkinson[1*]

[1]Department of Chemistry, University of Montreal, Montreal, QC H3C 3J7, Canada
[2]Department of Chemical Engineering, McGill University, Montreal, QC H3A 0C5, Canada
[3]Nu Instruments, Wrexham LL13 9XS, United Kingdom
[4]Department of Civil and Environmental Engineering, University of Alberta, Edmonton, AB T6G 1H9, Canada

* kj.wilkinson@umontreal.ca, ORCID: 0000-0002-7182-3624, Tel: +1 (514) 343-6741

ABSTRACT

Nanoparticle (NP) emissions to the environment are increasing as a result of anthropogenic activities, prompting concerns for ecosystems and human health. In order to evaluate the risk of NPs, it is necessary to know their concentrations in various environmental compartments, on regional and global scales; however, these data have remained largely elusive due to the analytical difficulties of measuring NPs in complex natural matrices. Here, we measure NP concentrations and sizes for Ti-, Ce- and Ag-containing NPs in numerous global surface waters and precipitation samples, and we provide insight into their compositions and origins (natural or anthropogenic). The results link NP occurrences and distributions to particle type, origin and sampling location. Based upon measurements from 46 sites across 13 countries, total Ti- and Ce-NP concentrations (regardless of origin) were often found to be within $10^4 - 10^7$ NP mL^{-1}, whereas Ag NPs exhibited sporadic occurrences with low concentrations generally up to 10^5 NP mL^{-1}. This generally corresponded to mass concentrations of <1 ng L^{-1} for Ag-NPs, <100 ng L^{-1} for Ce-NPs and <10 µg L^{-1} for Ti-NPs, given that measured sizes were often below 15 nm for Ce- and Ag-NPs and above 30 nm for Ti-NPs. In view of current toxicological data, observed NP levels do not yet appear to exceed toxicity thresholds for the environment or human health; however, NPs of likely anthropogenic origins appear to be already substantial in certain areas, such as urban centers. This work lays the foundation for broader experimental NP surveys, which will be critical for reliable NP risk assessments and the regulation of nano-enabled products.

2
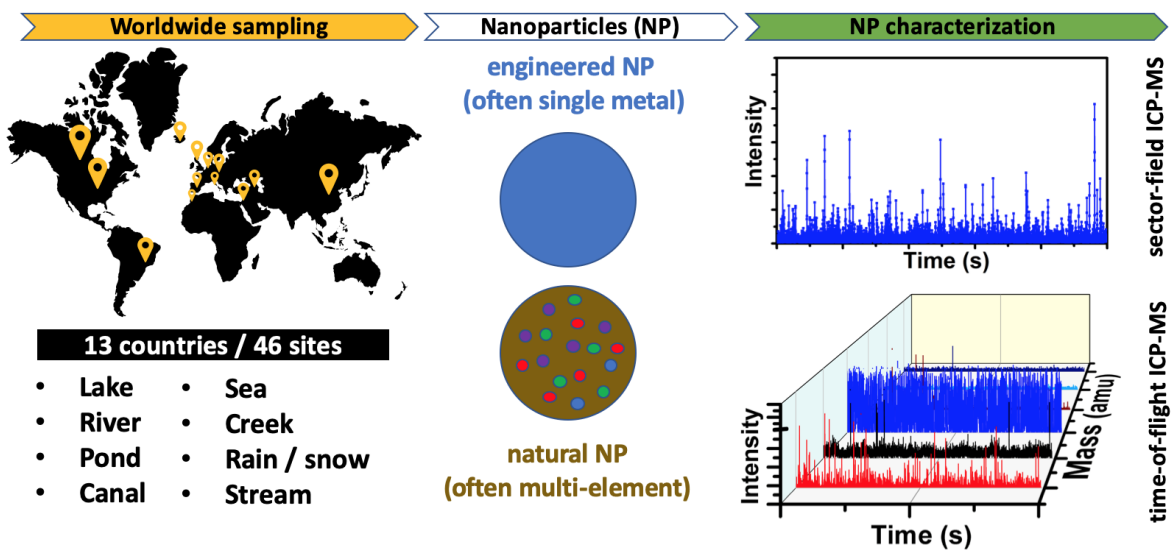
INTRODUCTION

Nanoparticles (NPs) are small (with three dimensions below 100 nm) particles that are found in many modern products and technologies and which are hypothesized to be in all environmental compartments.[1, 2] Although ***natural*** forms of NPs are ubiquitous,[3, 4] their impact on ecosystems and human health has really only been questioned in recent decades, coinciding with the increased production and disposal of ***engineered*** NPs.[1, 5, 6] Engineered NPs have been developed due to their generally enhanced chemical reactivities with respect to bulk materials of similar composition, which implies enhanced biological reactivity and potentially increased risk.[7]

To date, the vast majority of data on NP concentrations in the environment have been extrapolated from global production volumes[8] and (often assumed) product-release rates[9], generated through modelling[10] and based on contaminant transport patterns[11, 12]. Authors of these studies have systematically noted a very large uncertainty due to the poor quality of input data, the use of a large number of simplifying assumptions and the limited inclusion of environmental fate processes (*e.g.* agglomeration, heteroaggregation, dissolution, phase transformations). Although recently developed time-sensitive and size-specific probabilistic models[13, 14] represent a significant improvement, they may still overlook (i) the complexity of NP transformation or transport patterns; (ii) the time-dependence of input parameters; (iii) the role of geo-specific factors, *e.g.* scale, terrain, weathering; and (iv) the occurrences of episodic or localized events. Reliable risk assessments for the NPs will thus require experimental measurements[15-19] of the exposure concentrations, including spatially and temporally resolved data on their composition, size, and origin, across regions.[20] The near absence of NP measurements is due, in large part, to the analytical challenges of analyzing NPs in complex natural matrices, where NPs co-exist with various environmental colloids, particulates and dissolved molecules and ions, including natural organic matter.[21, 22]

73   Single-particle inductively coupled plasma mass spectrometry (SP-ICP-MS) is a promising state-

74   of-the-art technique, providing data on NP mass and number concentrations and size distributions.[23]

75   Indeed, recent developments with sector-field SP-ICP-MS have enabled the detection and

76   characterization of NPs with sizes down to a few nm (*i.e.* 3-4 nm for Ag- and CeO_2-NPs; 12 nm for

77   TiO_2-NPs).[18, 24, 25] The size detection limits (SDL) are critical since they provide the lower end of the

78   range of quantified NPs; NPs below the SDL are mistakenly classified as dissolved. Another important

79   aspect of nanoanalytics is the source discrimination of NPs, with the ultimate goal of quantifying

80   anthropogenic NP contributions. Given that anthropogenic NPs are often pure, while natural NPs tend

81   to exhibit chemical heterogeneities,[26-28] differences in particle compositions (*i.e.* purity, elemental

82   associations) have previously been used for source attribution of NPs. Fortunately, recent advances in

83   single-particle time-of-flight ICP-MS (SP-ICP-TOF-MS) have allowed whole elemental mass spectra

84   at sub-millisecond data acquisition rates, on a particle-by-particle basis.[29] These advances have paved

85   the way for experimental determinations of NPs in complex natural settings, providing information on

86   their mass/number concentrations, sizes, compositions and origins.

87   Here, we provide the first large-scale measurements of NPs for a wide range of surface waters

88   and precipitation samples that were collected from around the world. NP measurements were

89   performed using a high sensitivity sector-field ICP-MS and a prototype, high-speed ICP-TOF-MS.

90   They were focused on three NPs (Ag, TiO_2, CeO_2) that have suspected high anthropogenic

91   contributions[30]. The objectives were (i) to provide experimentally measured NP concentrations and

92   sizes; (ii) to explore NP composition and its link to NP size; and (iii) provide insight into the origin

93   (natural or anthropogenic) of the NPs. The data will be useful for modelling studies and risk

94   assessments and provide a baseline with respect to future determinations of environmental NPs.

95

96

MATERIALS AND METHODS

Global sampling campaign. Surface water and precipitation samples were collected at 46 sampling sites across 13 countries, including time-resolved measurements in Montreal (Quebec, Canada). The logistical challenges of conducting a large-scale sampling campaign were overcome with the help of 21 collaborators. In order to harmonize the sampling process, experimental material kits, as well as detailed sampling protocols were sent to each of the destinations in advance of the sampling date. Each kit contained, at a minimum, 50 mL polypropylene centrifuge tubes (Fisher Scientific) (10 used to collect triplicate rainwater samples), 15 mL polypropylene centrifuge tubes (Fisher Scientific) (>3 per sample), 20-30 mL syringes with no rubber gaskets (Henke-Sass Wolf, Germany)) (>3 per sample), 0.45-μm 33 mm PVDF (polyvinylidene fluoride) syringe filters (Sigma-Aldrich) (>3 per sample), Parafilm^{TM} M wrapping films (Fisher Scientific) and a few pairs of non-powdered nitrile gloves (Kimberley-Clark).

Surface water samples were collected from the top 5-10 cm and immediately filtered on-site using the PVDF filters, which were pre-rinsed[29] with ~6 mL of the sample (corresponds to >50x filter void volume) in order to minimize sorptive losses. Higher volumes were avoided to minimize the risk of concentration polarization artefacts on the filter membrane. Sample filtrate was then added to triplicate 15 mL tubes, to the brim. The filtration step was designed to assist with the preservation of the samples during transport by removing most microbes and large particles. Based upon measured sizes and particle numbers, the NP appeared to be stable for at least 12 days (Fig. S1).

Precipitation (rain) samples were collected by leaving out 6-8 of the 50 mL centrifuge tubes (>0.5 m above the ground) during rainfall events. In order to avoid/minimize sample evaporation and dry deposition of atmospheric (nano)particles, the duration of rain collection was limited to a single precipitation event and to <2 hours. The collected rain fractions were then combined into triplicate 15 mL tubes (filled to the brim). All tubes were labeled, and sampling geo coordinates were recorded.

121   The tubes were then sealed with parafilm, placed into a padded envelope, and express delivered to the

122   Montreal laboratory (typically, 1-2 days for Canada; 3-4 days for Europe, USA and Brazil; 7-12 days

123   for China). Once received, samples were refrigerated at 4 °C until analysis.

124   **Sample preparation for analysis**. Precipitation samples, on the day of their arrival in the lab, were

125   ultrasonicated for 30 minutes (Branson Ultrasonic Cleaner, 5510R-DTH Model, 135 W, 42 kHZ ± 6%)

126   and then filtered using 0.45 µm poresize PVDF filters that had been pre-rinsed with 6 mL of sample.

127   On the day of analysis, all filtered samples (surface or precipitation) were treated with 10 min of

128   ultrasonication, and then, if necessary, were diluted 5-50x for measurements by ICP-MS.

129   **SP-ICP-MS measurements**. SP-ICP-MS data were acquired on a double-focusing sector-field ICP-

130   MS (AttoM ES, Nu Instruments, United Kingdom), at low resolution (300) and using single ion

131   acquisition, in fast scan mode.[24] While Ce-NP analysis could be optimally performed using a wet

132   aerosol[18], for Ti- and Ag-NP analysis, the sensitivity was further enhanced by coupling the ICP-MS to

133   a desolvator (Aridus II, Teledyne Cetac Technologies) that used a PFA (perfluoroalkoxy) micro-flow

134   nebulizer (self-aspiration rate of 200 µL min^{-1} for 1 L min^{-1} of Ar)[29]. The flow rates of the nebulizer

135   gas (argon) and membrane sweep gas (argon) typically ranged between 0.7-1.0 L min^{-1} and 3-7 L min^{-1},

136   respectively. As per previously optimized strategies[18, 24], ^{49}Ti, ^{140}Ce and ^{107}Ag were measured during

137   the analysis. Notably, the choice of ^{49}Ti was predicated on the fact that, despite its low abundance, it

138   has fewer interferences, and its analysis was enabled by the high-sensitivity system. Data acquisition

139   spanned 50 s with an optimized dwell time of 50 µs, resulting in ca. 10^6 datapoints per replicate. This

140   yielded SDLs of ~15 nm for TiO$_2$, and ~4 nm for CeO$_2$ and Ag NPs[18, 24, 29]. Sensitivity calibrations

141   were determined based on ionic standards of Ti, Ce and Ag (High Purity Standards). Transport

142   efficiencies (TE) were determined by the particle frequency method[31] using ultra-uniform 30 nm Au

143   NPs (NanoComposix, AUXU30-1M) with a known particle number concentration. TE measurements

144   were validated with a second standard reference material (60 nm Au NPs, NIST 8013). TE values

145 typically ranged between 0.11-0.15 µL s^{-1} or 3.5-4.5 % for Ce analysis (*i.e.* wet mode) and 0.45-0.55

146 µL s^{-1} or 13-15% for Ti and Ag analysis (*i.e.* dry mode). Wherever necessary, filtered samples were

147 diluted (1-50x) to minimize the incidences of concurrent peaks (< 10,000 events or 1% of total

148 datapoints), while ensuring a statistically significant number of NPs. Detection thresholds of ~360 NP

149 mL^{-1} Ti-NPs, 1500 NP mL^{-1} Ce-NPs and 900 NP mL^{-1} Ag-NPs could be established by requiring that

150 the peak numbers collected over a 50 s acquisition exceeded those in the blanks by at least a factor of

151 3.[32]

152 **SP-ICP-TOF-MS measurements**. SP-ICP-TOF-MS data were acquired on a prototype high-speed

153 time-of-flight ICP-MS (Nu Vitesse, Nu Instruments, United Kingdom) that enabled the

154 characterization of multi-element particles on a particle-by-particle basis.[29] The instrument was

155 equipped with a segmented reaction cell, into which ca. 4-6 cm^3 min^{-1} of He and ca. 4 cm^3 min^{-1} of H_2

156 gas were introduced to eliminate argon and nitrogen-based interferences (*e.g.* for elements such as K,

157 Ca, Cr, Fe and Si). To further increase the sensitivity, the instrument was coupled to an Aridus II

158 desolvator (Teledyne Cetac Technologies), with similar nebulizer gas (argon) and sweep gas (argon)

159 conditions as were used for the sector-field instrument. Signal acquisitions were performed every 25.5

160 µs for a near full range of time of flight mass spectra (23-238 amu), continuously and with no loss of

161 data. Following the accumulation of 3 consecutive acquisitions, electronic noise was subtracted, and

162 signals were integrated and individually stored for each isotope (*i.e.* from Na to U every 76 µs). Total

163 sampling time ranged between 0.5-10 min and was adjusted according to particle numbers in the

164 samples (*i.e.* to achieve statistically significant particle counts). Sensitivity calibrations were built

165 following the analysis of custom-prepared multi-element standards (CLMS-1, CLMS-2, CLMS-3 and

166 CLMS-4, SPEX CertiPrep). TEs were determined using the particle size method[31] and were based on

167 ionic Au sensitivities and an ultra-uniform NP standard of 30 nm (NanoComposix, AUXU30-1M). For

168   NPs considered to be composed of a single metal, SDLs on the ICP-TOF-MS corresponded to ~30 nm

169   (TiO$_2$) and ~16 nm (CeO$_2$ and Ag).

170   **Data processing for SP-ICP-MS/SP-ICP-TOF-MS**. SP-ICP-MS data was processed using Nu Quant

171   software version 2.2 (Nu Instruments, United Kingdom), as previously described in Hadioui *et al*.

172   (2019)[24] and Shaw and Donard (2016)[33]. Briefly, the data processing algorithm used data smoothing

173   to reduce background fluctuations for time-resolved raw data. A rolling search window was created at

174   time zero, where the algorithm searched for a peak maximum and set its pre- and post-inflection points.

175   Once found, the window was shifted in order to detect more peaks – a process that spanned the whole

176   data acquisition period. For each detected peak, the local background was calculated based on the

177   stored inflection point data. It was then subtracted from the integrated raw data for the peak (further

178   details in the SI). The average of local backgrounds (*i.e*. global background) was used to calculate

179   dissolved metal content or interferences. NP masses and sizes were calculated based on ionic

180   sensitivities and TE measurements, while assuming spherical shapes and particle densities of 4.23, 7.13

181   and 10.49 g cm^{-3} for TiO$_2$, CeO$_2$ and Ag NPs, respectively.

182   SP-ICP-TOF-MS data was processed using a modified version of NuQuant software (NuQuant

183   Vitesse prototype, Nu Instruments, United Kingdom).[29] The software algorithm used similar

184   smoothing and peak detection parameters, as for the single-isotope analysis, however, it searched for

185   multiple target isotopes (*e.g*. ^{48}Ti, ^{27}Al, ^{56}Fe for Ti-, Al- and Fe-containing NPs) simultaneously,

186   determining start and end timestamps for each particle event. Based on the timestamps, counts for all

187   isotopes were then identified. Given the full width half maximum (FWHM) values and the baseline

188   standard deviations, a noise threshold was applied to filter out background artifacts, often arising from

189   high-background metals (*e.g*. Na, Ca, Zn). While FWHM values were used to screen potential peak

190   artifacts, the rapid monitoring of NPs was also conducted by sorting the detected NP peaks by isotope

191   type and intensities in order to focus on peaks of potential concern, *i.e*. very slender or very wide peaks

192　with low intensity). NP masses were calculated based on multi-element calibrations and TE

193　measurements.

194　**RESULTS AND DISCUSSION**

195　**NP occurrence and concentrations across the globe**. Concentrations of Ti-, Ce-, and Ag-containing

196　NPs are presented for both surface waters and precipitation (Fig. 1) for a wide geographical range of

197　samples (further details in Tables S1, S2, S3 and S4). Samples from 46 sites across 13 countries were

198　analyzed, representing an array of natural and artificial water bodies, including lakes, rivers, ponds,

199　canals, coastal marine water and natural precipitation, and encompassing a wide range of water types

200　(*i.e*. salinities, natural organic matter content, hydrodynamic regimes). La-containing NPs were also

201　reported (Fig. S2) to provide additional insight into particle origins. Based upon global production

202　volumes[1, 2, 8], we would expect La-containing NPs to be predominantly from natural sources, Ce- and

203　Ti-NPs to be from both natural and anthropogenic sources and Ag-NPs to be predominantly from

204　anthropogenic sources.

205　　　It is notable that NP concentrations varied substantially with respect to both sampling location

206　and NP type. For example, while Ti- and Ce-NP concentrations in surface and precipitation waters

207　typically ranged between $10^4 – 10^6$ NP mL^{-1}, Ag-NPs were often below detection limits of 900 NP

208　mL^{-1} and were only seldomly measured in the higher concentration range of $10^4 – 10^5$ NP mL^{-1}. Among

209　the sampling sites examined, Ti-NPs were at the lowest concentrations in the Canadian far north

210　(Yukon territories), whereas snow samples from the Sólheimajökull glacier (Iceland) contained the

211　greatest number of particles (Fig. 1). While low NP concentrations were intuitively expected for

212　samples relatively less impacted by urban/industrial activities (*e.g.* Yukon), in the absence of particle

213　influx due to long-range transport,[5, 11] the observed high NP concentrations of Iceland demonstrated

214　the region-specific nature of NP emissions. Indeed, the geographical position of the Sólheimajökull

215 glacier between two volcanoes (Eyjafjallajökull and Katla) renders it vulnerable to volcanically

216 generated particulate pollution, which is known to contain Fe and Ti.[34, 35]

217   Ce-NPs generally followed a similar distribution pattern to that of the Ti-NPs, except in the

218 case of the marine samples. While this may have been caused by significant particle agglomeration and

219 sedimentation (potentially due to charge screening),[36] it is nonetheless puzzling that Ti-NPs were not

220 subjected to a similar fate. It is possible that this observation is related to particle-specific properties

221 of the NP. For example, TiO_2 NPs have been shown previously to partition into the top (more

222 hydrophobic) layers of surface waters rather than remain uniformly distributed in the water column[37].

223 When compared to La-NPs (Fig. S2), which often hovered around 10^6 NP mL^{-1}, Ti- and Ce-NP

224 concentrations exhibited substantially more variability across sampling locations, likely caused by

225 larger and more variable anthropogenic contributions of these two NPs. Furthermore, Ag-NPs showed

226 concentration trends that were vastly different from both Ti- and Ce-NPs. Given that Ag is much less

227 abundant on Earth as compared to Ti or Ce, one could hypothesize that its concentration is more

228 influenced by anthropogenic processes – such as incineration/burning, metal smelting or mining

229 activities.[38, 39] The observation that Ag-NP concentrations were often below detection limits (900 NP

230 mL^{-1}) but with maxima in the range of $\sim 10^4$ NP mL^{-1} is indeed consistent with their input via

231 anthropogenic sources[19] – probably as a result of localized pollution or episodic events – and their low

232 thermodynamic stabilities[40].

233   NPs are thought to be scavenged by rainwaters, so concentrations in rain will also depend

234 greatly on the frequency and duration of precipitation events, preceding the sampling. While it is

235 difficult to speculate on the sources of the Ag NPs in the precipitation, the high concentrations observed

236 in the Hohhot (CHN) rain sample are nonetheless consistent with China currently being the largest

237 producer of silver in the Asia Pacific.
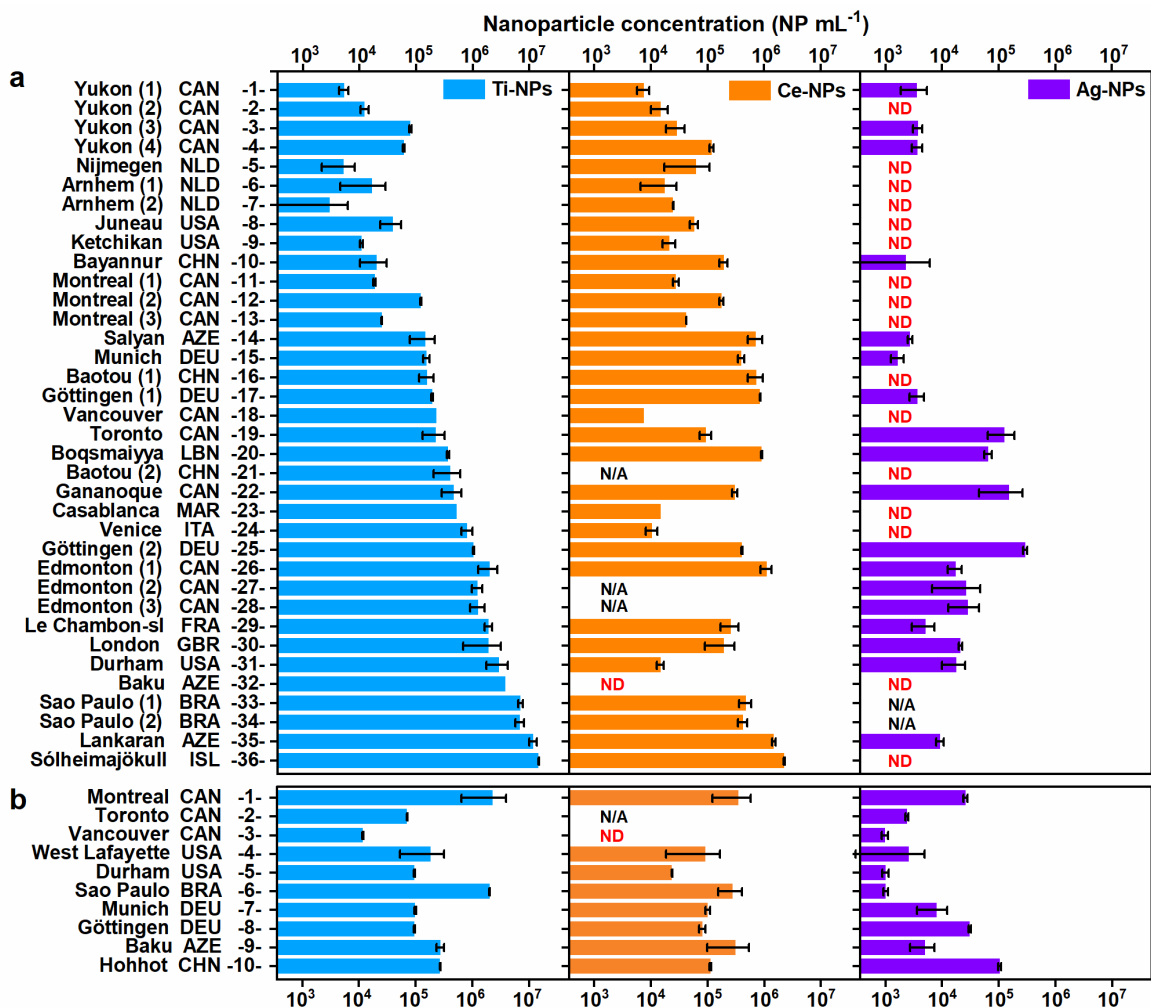
Figure 1. Nanoparticle concentrations in global surface waters and precipitation. Particle number concentrations for Ti-, Ce- and Ag-containing NPs (denoted by blue, orange and violet bars, respectively) collected at 46 sampling sites across 13 countries and measured in surface waters (**a**) and precipitation (**b**). Sampling sites are indicated by city/province names and ISO country codes. Measurements were performed using a sector-field ICP-MS. ND stands for "not detected" and refers to concentrations below the detection limits of the technique (ca. 1500 NP mL^{-1} for Ce and ca. 900 NP mL^{-1} for Ag). N/A refers to samples that were not analyzed. Error bars represent the standard deviations of triplicate samples.

The measurements presented here represent punctual determinations of NP concentrations and size distributions that are continually subjected to environmental factors, including precipitation, temperature, freeze-thaw, wind and episodic NP emission or transport events. Indeed, measurements of Ti- and Ce-containing NPs measured in Montreal surface waters over 5 weeks (Fig. S3) showed that NP concentrations fluctuated by ~2-5x and appeared to be affected by the frequency/duration of

11

251   precipitation events. For example, higher concentrations of Ti- and Ce-NP were observed immediately

252   after significant rain events and were potentially related to increased urban run-off[41].

253   **NP composition and origins.** Select international locations were used to explore the source of the Ti-

254   NPs using SP-ICP-TOF-MS. Particle purity was used as an indicator of particle origin[3, 27], under the

255   assumption that anthropogenic NPs often occur as pure particles, whereas naturally occurring NPs

256   often contain multiple elements. While the purity assumption is not a rigorous criterion for determining

257   NP source, it can provide insight into particle origin when coupled with data on individual elemental

258   associations and region-specific pollution scenarios. Multi-element analyses of the Ti-NPs in

259   precipitation (Fig. 2a) showed that the NPs exhibited a range of complex associations with other metals.

260   For example, for 80% of the Ti-NPs detected in Sao Paulo and Montreal rainwaters, only Ti could be

261   detected (*i.e.* >99.9 % Ti), whereas this fraction dropped to about 50% for rainwater samples collected

262   in Munich or Durham and to <30% for samples collected from Vancouver and Sólheimajökull.

263   Associations with specific elemental tracers, such as Al, Si and Fe (*i.e.* aluminosilicates)[16, 42, 43] were

264   particularly enlightening. For example, in the precipitation from Sao Paulo and Montreal, Ti-containing

265   NPs were found more frequently than Al-, Si- and Fe-containing NPs (Fig. 3a,b). Furthermore, Al, Si

266   or Fe could only be detected in a small fraction (<10%) of the Ti-containing NPs (Fig. 3c,d), reinforcing

267   the contention that there may have been a substantial anthropogenic input of Ti-NPs.[44] In contrast, for

268   the Vancouver rainwater, Ti-NPs were overwhelmingly less present than the Si- and Fe-containing

269   NPs (Fig. 3a,b), with a majority of the Ti-containing NPs (>90%), also containing Si, Fe and Al (Fig.

270   3c,d). For the sample from the Sólheimajökull glacier, Ti-NPs were predominantly enriched with Fe

271   (70% of cases), occasionally with Al (15%) and very rarely with Si (1%) – an observation that is

272   consistent with this environment being a major sink/carrier for natural Fe-containing nanominerals.[4,
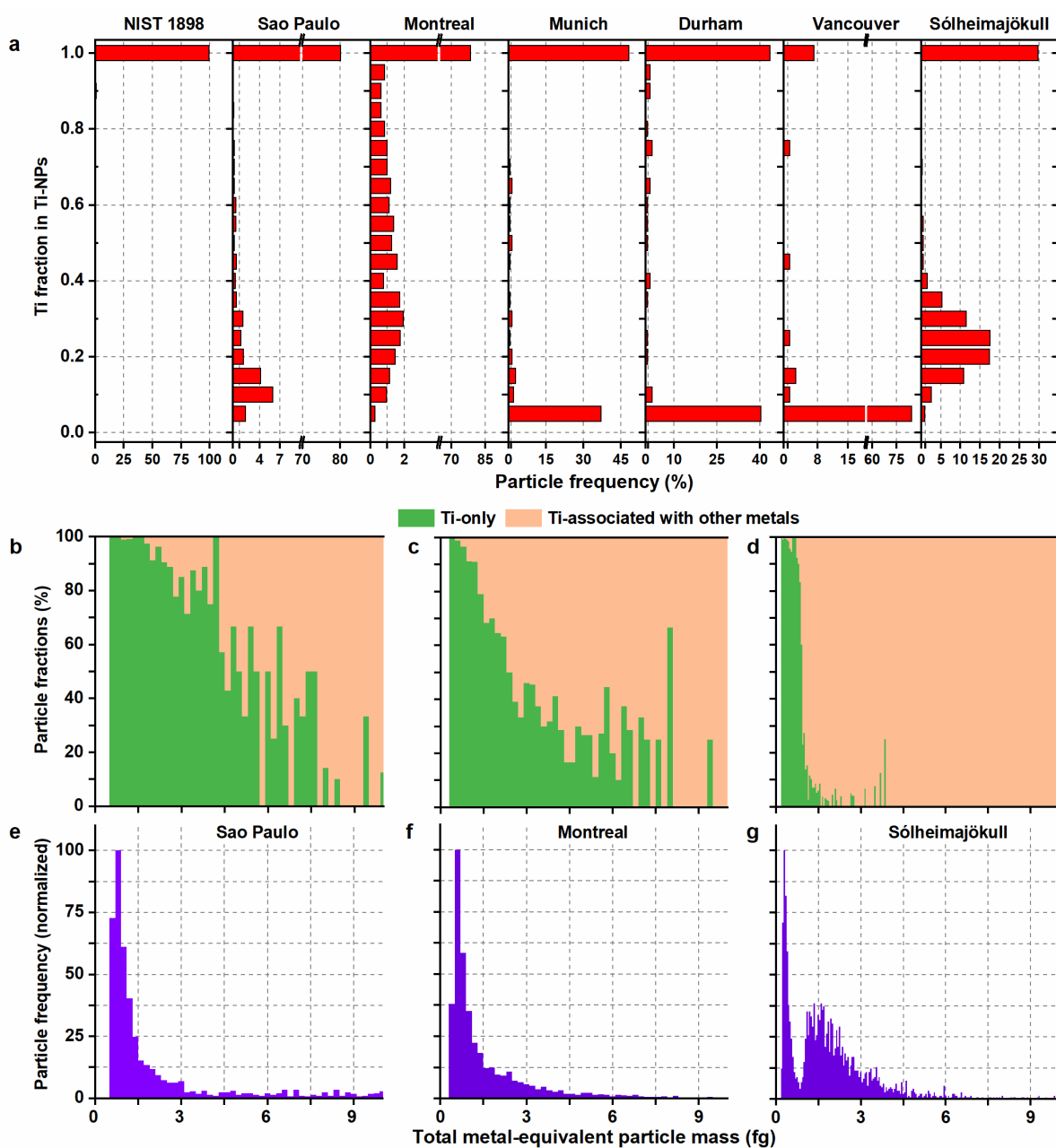
273   45]

Figure 2. Particle compositions and their link to particle masses (or sizes). a, Ti fractions in Ti-containing particles as determined in TiO_2 nanoparticle standard (NIST 1898) and in natural precipitation samples collected at six locations: Sao Paulo (BRA), Montreal (CAN), Munich (DEU), Durham (USA), Vancouver (CAN) and Sólheimajökull (ISL). **b-g,** In selected samples of Sao Paulo, Montreal and Sólheimajökull, each Ti-particle is identified as containing 'only Ti' or 'Ti with additional metals/metalloids' and the corresponding number fraction (%) (**b-d**) of these particle categories as a function of total metallic particle mass (*i.e.* distributions, **e-f**) are reported. All calculations are based on data that was collected using single-particle ICP-TOF-MS.

282
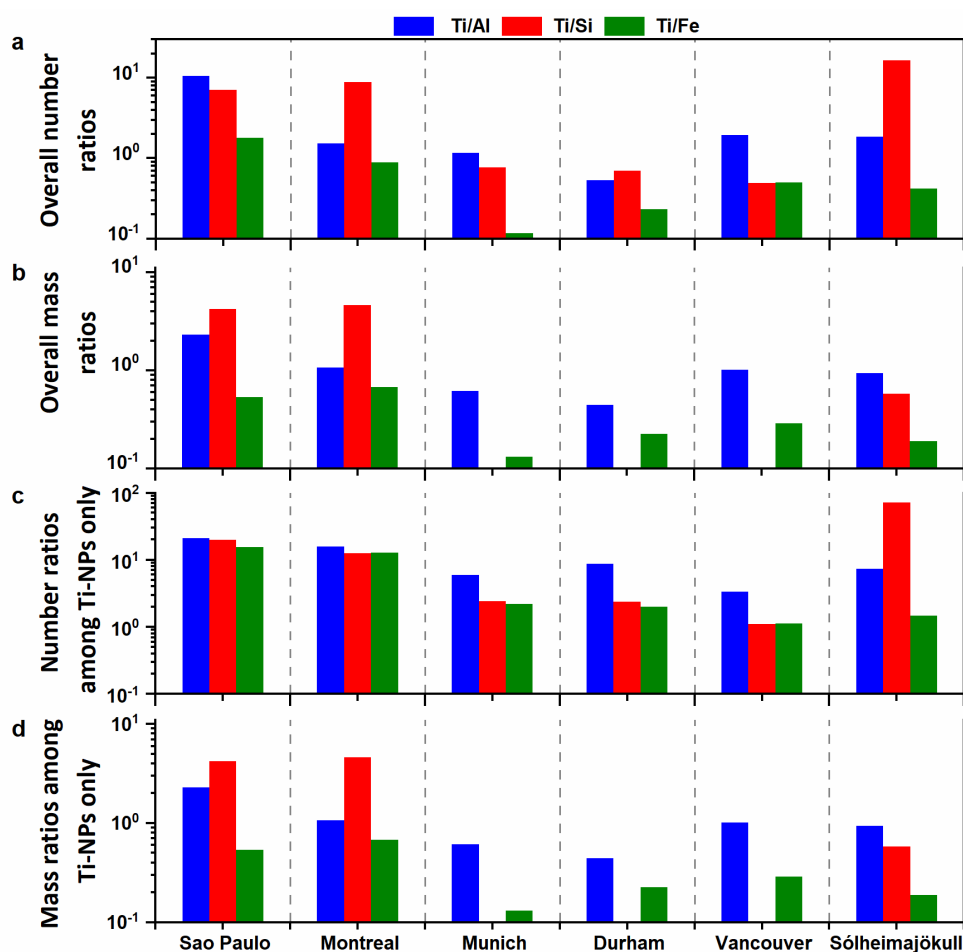
Figure 3. Metallic associations of nanoparticles on a single particle level. a, Ratios of the number of Ti-containing NPs to the number of Al-, Si- or Fe-containing NPs. **b,** Ratios of Ti mass to mass of Al, Si or Fe in the NP. **c,** Ratios of the number of Ti-containing NPs to the number of those both Ti-Al, Ti-Si or Ti-Fe. **d,** Ratios of the total mass of Ti in Ti-containing NPs to that of the Al, Si or Fe. Blue, red, and green bars denote Ti/Al, Ti/Si and Ti/Fe (mass or number) ratios, respectively. When these ratios are below 0.1 (*i.e.* low cut-off on y-axis), bars were not visible, meaning that the second metal (Al, Si or Fe) was much more present as compared to Ti. Calculations are performed for natural precipitation samples from Sao Paulo (BRA), Montreal (CAN), Munich (DEU), Durham (USA), Vancouver (CAN) and Sólheimajökull (ISL). Measurements were performed using single particle ICP-TOF-MS.

NP sizes and origins. Equivalent diameters were calculated based upon the assumption that NPs were

spherical and contained only TiO_2, CeO_2 or Ag. In that case, there was significant overlap in the size

distributions of the respective NPs in the different surface waters, with modes for the diameters often

occurring at ~30-60 nm for the Ti-NPs and below 20 nm for the Ce-NPs and Ag-NPs (note the detection

limits of ~15 nm for TiO_2, ~4 nm for CeO_2 and Ag; example distributions are provided in Fig. 4a; mean

sizes in Fig. 4b,c). Nonetheless, particle sizes appeared to be affected by the sample nature. For

14

example, mean diameters of Ti- and Ce-NPs detected in the rivers and rains were generally larger than those found in artificial water bodies, such as ponds and canals, or saline waters (Fig. 4b,c). This tendency may have been dictated by a combination of physiochemical (*e.g.* ionic strength, natural organic matter, redox conditions) and hydrodynamic (*i.e.* turbulence in water) factors and the way different NP types respond to them. Another notable source of variability is that the location of some of the water bodies might have favored the influx of certain types of NPs. For example, the observation of smaller NP sizes in artificial water bodies (*e.g.* ponds, canals) is consistent with the fact that these waters are mainly found in urban environments, which render them more susceptible to pollution with anthropogenic NPs (which generally tend to be smaller).
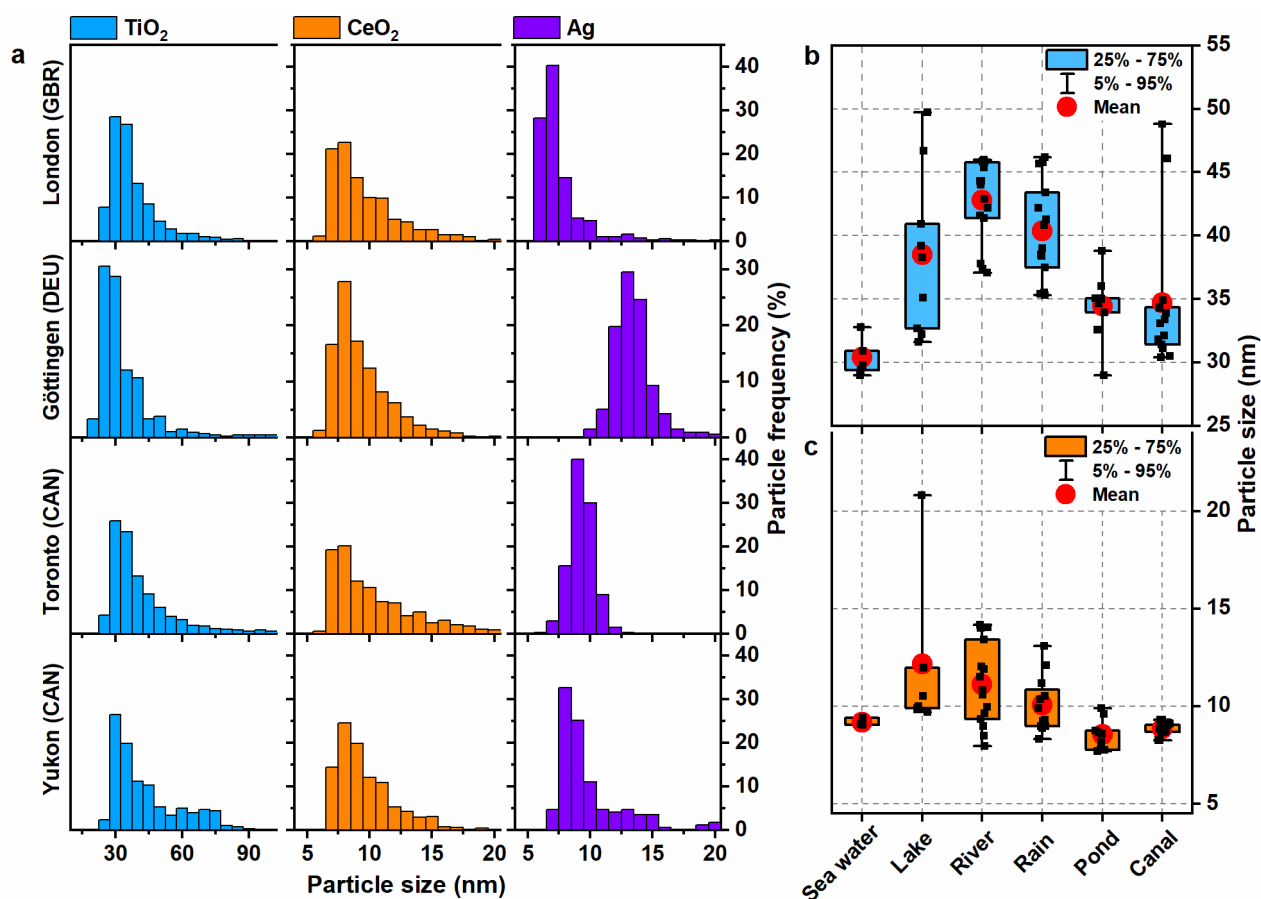
Figure 4. Nanoparticle size distributions and mean sizes by water type. a. Particle size distributions as determined for Ti-, Ce- and Ag-containing NPs in London (The Long Water Lake), Göttingen (Leine River), Toronto (Lake Ontario) and Yukon (Kluane Lake) surface waters. Measured (mean) sizes for Ti- (**b**) and Ce-containing (**c**) NPs detected in 46 samples. Samples were categorized by water type. Limits of the boxes and

15

312 whiskers represent 25%-75% and 5%-95% percentiles, respectively. Red solid circles represent the mean sizes,
313 observed within each water category. NP measurements were performed using a sector-field ICP-MS. For all
314 determinations, particle sizes were calculated by assuming that Ti-, Ce- and Ag-containing NPs occurred solely
315 in the forms of spherical TiO_2, CeO_2 and Ag, respectively.

316   While the above estimates are relevant for pure NP populations, sizes for multi-element NPs

317 are more complicated to calculate (Fig. S4) due to an uncertainty on the particle densities and the

318 unquantified contribution of several elements in the NPs (*e.g*. oxygen, halogens). For size estimates

319 determined by taking into account the multi-elemental nature of particles, it was possible to observe

320 two distinct peaks in the particle size distribution (*e.g*. Fig. S4 for the Icelandic sample). When the NPs

321 were profiled as a function of their purity, only Ti (<1 fg per NP) was detected in the peak of the smaller

322 NPs, whereas the peak corresponding to larger NPs systematically contained multiple elements (Fig.

323 2d,g). Similar observations were made for samples from Sao Paulo (Fig. 2b,e) and Montreal (Fig. 2c,f),

324 where the smallest NPs were generally of much higher purity as compared to the larger NPs. Although

325 it might be possible to attribute the absence of small multi-element NPs to instrumental detection limits

326 (Fig. S5), it was nonetheless extremely rare to find pure Ti-NPs (oxides) among the larger particles.

327 Such results show, as has often been assumed in the literature, that the anthropogenically generated

328 NPs tend to be smaller and purer particles.

329 **Global environmental implications.** These results represent the first large-scale experimental

330 determinations of NPs in surface waters and precipitation, encompassing three major NPs that are

331 known to be emitted as a result of human activities. Data clearly show that NPs, whether anthropogenic

332 or natural, have reached far corners of the world, albeit at concentrations that are dependent on the

333 nature of the NPs, the geographical sampling location and the sampling time. Ti- and Ce-NP

334 concentrations, which were impacted by both natural and anthropogenic inputs, showed the greatest

335 variability across regions, ranging between 10^4-10^7 NP mL^{-1}. In contrast, the sporadic nature of the Ag

336 NPs, and their generally lower concentrations (up to 10^5 NP mL^{-1}), showed that while anthropogenic

337 (episodic) inputs of Ag NPs are occurring, they are likely still relatively infrequent or low concentration

338   events. For all NPs, particle concentrations and sizes were influenced by the water type, the nature of

339   the sampling location and short- or long-range particle transport. Regardless of their nature, NP

340   concentrations were often below 10^6 NP mL^{-1} (*i.e.* <1 ng L^{-1} for Ag-NPs; <100 ng L^{-1} for Ce-NPs; <10

341   µg L^{-1} for Ti-NPs), which are levels that presently do not appear to pose a high risk to

342   ecotoxicological[46-48] or human health[49].

343   In spite of the challenges of quantitatively distinguishing NPs with respect to their origins, the

344   determinations of particle purity and size presented here indicated that smaller and purer NPs of

345   possibly anthropogenic origin may indeed already dominate certain environments, such as large urban

346   centers. It is worth noting that anthropogenic NPs are not only limited to the engineered NPs (*i.e.*

347   manufactured), as they may also include NPs that are incidentally generated as a result of

348   anthropogenic processes.[5] For example, magneli phase titania (Ti$_x$O$_{2x-1}$), while rarely present in

349   geological settings, was recently shown[50] to be emitted from industrial coal burning, since Ti-minerals

350   are an essential part of coal (*i.e.* >0.1 wt%). Consequently, while we do not have control over the spread

351   of natural NPs, the increased industrialization and use of nanomaterials is likely to lead to the increased

352   release and distribution of the smaller (and likely more biologically available) anthropogenic NPs at

353   concentrations that exceed those of natural NPs. This will increasingly contribute to added

354   ecotoxicological stress.

355   While the analytical measurements were state-of-the-art, it is nonetheless extremely important

356   to point out that the data were only a snapshot of a single sampling day at a given location. It is thus

357   highly speculative to compare multiple sites or make inferences on the sources of the NPs, without

358   complementary data on the spatial or temporal variations at a given site. Indeed, spatiotemporal

359   distributions of NPs are likely impacted by geo-meteorological factors (*e.g.* geochemistry, terrain,

360   precipitation, air currents), as well as numerous transformational processes that are occurring and

361   which are influenced by the physicochemistry of the media, including pH, ligand concentrations and

362 redox potential. This can lead to highly variable distributions of NPs, even on limited spatial scales.

363 Indeed, the concentration of Ag NPs collected from Kiessee Lake (pond) in Göttingen (DEU), which

364 was formerly a quarry pit, contained almost two orders of magnitude more Ag NPs, as compared to a

365 sample from the Leine River (Fig. 1), even though sampling spots were within 2 km of each other. This

366 observation suggests that in the absence of analytical data, it will be very difficult for large scale models

367 to account for important short-range or on-site contributions of the NPs.

368 This work lays the foundation for more thorough experimental measurements of NPs, which

369 can be used as both input data and to validate models being developed to assess the risk of NP. Future

370 technical improvements to the sensitivity of analysis techniques, particularly for the multi-element

371 analysis of single nanoparticles – aided by isotopic fingerprinting using machine learning[51, 52] – will

372 pave the way for the full quantitative profiling of the NPs by origin. This will in turn enable a more

373 quantitative evaluation of the impact of burgeoning nanotechnology industries on local, regional and

374 global scales.

375 **ASSOCIATED CONTENT**

376 The supporting information is available free of charge at: xxx

377 Additional details on data processing, particle stability, La NP concentrations, time-resolved

378 measurements, modelled size distributions, method detection limits, sampling information and NP

379 mass concentrations (PDF).

380

390   **COMPETING INTERESTS**

391   PS is an employee of Nu Instruments (United Kingdom). The other authors declare no competing

392   interests.

393

394   **REFERENCES**

395   1.   Keller, A. A.; McFerran, S.; Lazareva, A.; Suh, S., Global life cycle releases of engineered
396   nanomaterials. *Journal of nanoparticle research* **2013,** *15* (6), 1692.
397   2.   Vance, M. E.; Kuiken, T.; Vejerano, E. P.; McGinnis, S. P.; Hochella Jr, M. F.; Rejeski,
398   D.; Hull, M. S., Nanotechnology in the real world: Redeveloping the nanomaterial consumer
399   products inventory. *Beilstein journal of nanotechnology* **2015,** *6* (1), 1769-1780.
400   3.   Hochella, M. F.; Lower, S. K.; Maurice, P. A.; Penn, R. L.; Sahai, N.; Sparks, D. L.;
401   Twining, B. S., Nanominerals, mineral nanoparticles, and earth systems. *science* **2008,** *319* (5870),
402   1631-1635.
403   4.   Maddenc, A. S., Naturally Occurring Inorganic Nanoparticles: General Assessment and a
404   Global Budget for One of Earth's Last Unexplored Major Geochemical Components. *Nature's*
405   *Nanostructures* **2012**, 1.
406   5.   Hochella, M. F.; Mogk, D. W.; Ranville, J.; Allen, I. C.; Luther, G. W.; Marr, L. C.;
407   McGrail, B. P.; Murayama, M.; Qafoku, N. P.; Rosso, K. M., Natural, incidental, and engineered
408   nanomaterials and their impacts on the Earth system. *Science* **2019,** *363* (6434), eaau8299.
409   6.   Nowack, B.; Ranville, J. F.; Diamond, S.; Gallego-Urrea, J. A.; Metcalfe, C.; Rose, J.;
410   Horne, N.; Koelmans, A. A.; Klaine, S. J., Potential scenarios for nanomaterial release and
411   subsequent alteration in the environment. *Environmental toxicology and Chemistry* **2012,** *31* (1), 50-
412   59.
413   7.   Auffan, M.; Rose, J.; Bottero, J.-Y.; Lowry, G. V.; Jolivet, J.-P.; Wiesner, M. R., Towards
414   a definition of inorganic nanoparticles from an environmental, health and safety perspective. *Nature*
415   *nanotechnology* **2009,** *4* (10), 634.
416   8.   Kuenen, J.; Pomar-Portillo, V.; Vilchez, A.; Visschedijk, A.; van der Gon, H. D.;
417   Vázquez-Campos, S.; Nowack, B.; Adam, V., Inventory of country-specific emissions of engineered
418   nanomaterials throughout the life cycle. *Environmental Science: Nano* **2020**.

419   9.   Sun, T. Y.; Mitrano, D. M.; Bornhöft, N. A.; Scheringer, M.; Hungerbühler, K.; Nowack,
420   B., Envisioning nano release dynamics in a changing world: using dynamic probabilistic modeling to
421   assess future environmental emissions of engineered nanomaterials. *Environmental science &*
422   *technology* **2017,** *51* (5), 2854-2863.
423   10.   Song, R.; Qin, Y.; Suh, S.; Keller, A. A., Dynamic model for the stocks and release flows of
424   engineered nanomaterials. *Environmental science & technology* **2017,** *51* (21), 12424-12433.
425   11.   Prospero, J. M., Long-range transport of mineral dust in the global atmosphere: Impact of
426   African dust on the environment of the southeastern United States. *Proceedings of the National*
427   *Academy of Sciences* **1999,** *96* (7), 3396-3403.
428   12.   Praetorius, A.; Tufenkji, N.; Goss, K.-U.; Scheringer, M.; von der Kammer, F.; Elimelech,
429   M., The road to nowhere: equilibrium partition coefficients for nanoparticles. *Environmental*
430   *Science: Nano* **2014,** *1* (4), 317-323.
431   13.   Zheng, Y.; Nowack, B., Size-Specific, Dynamic, Probabilistic Material Flow Analysis of
432   Titanium Dioxide Releases into the Environment. *Environmental Science & Technology* **2021,** *55*
433   (4), 2392-2402.
434   14.   Nowack, B.; Baalousha, M.; Bornhöft, N.; Chaudhry, Q.; Cornelis, G.; Cotterill, J.;
435   Gondikas, A.; Hassellöv, M.; Lead, J.; Mitrano, D. M., Progress towards the validation of modeled
436   environmental concentrations of engineered nanomaterials by analytical measurements.
437   *Environmental Science: Nano* **2015,** *2* (5), 421-428.
438   15.   Gondikas, A. P.; Kammer, F. v. d.; Reed, R. B.; Wagner, S.; Ranville, J. F.; Hofmann, T.,
439   Release of TiO2 nanoparticles from sunscreens into surface waters: a one-year survey at the old
440   Danube recreational Lake. *Environmental Science & Technology* **2014,** *48* (10), 5415-5422.
441   16.   Loosli, F.; Wang, J.; Rothenberg, S.; Bizimis, M.; Winkler, C.; Borovinskaya, O.;
442   Flamigni, L.; Baalousha, M., Sewage spills are a major source of titanium dioxide engineered (nano)-
443   particle release into the environment. *Environmental Science: Nano* **2019,** *6* (3), 763-777.
444   17.   Peters, R. J.; van Bemmel, G.; Milani, N. B.; den Hertog, G. C.; Undas, A. K.; van der
445   Lee, M.; Bouwmeester, H., Detection of nanoparticles in Dutch surface waters. *Science of the Total*
446   *Environment* **2018,** *621*, 210-218.
447   18.   Jreije, I.; Azimzada, A.; Hadioui, M.; Wilkinson, K. J., Measurement of CeO2 Nanoparticles
448   in Natural Waters Using a High Sensitivity, Single Particle ICP-MS. *Molecules* **2020,** *25* (23), 5516.
449   19.   Wang, J.-L.; Alasonati, E.; Tharaud, M.; Gelabert, A.; Fisicaro, P.; Benedetti, M. F., Flow
450   and fate of silver nanoparticles in small French catchments under different land-uses: The first one-
451   year study. *Water Research* **2020**, 115722.
452   20.   Svendsen, C.; Walker, L. A.; Matzke, M.; Lahive, E.; Harrison, S.; Crossley, A.; Park, B.;
453   Lofts, S.; Lynch, I.; Vázquez-Campos, S., Key principles and operational practices for improved
454   nanotechnology environmental exposure assessment. *Nature Nanotechnology* **2020,** *15* (9), 731-742.
455   21.   Corsi, I.; Bergami, E.; Grassi, G., Behavior and bio-interactions of anthropogenic particles in
456   marine environment for a more realistic ecological risk assessment. *Frontiers in Environmental*
457   *Science* **2020,** *8*, 60.
458   22.   Cornelis, G.; Hund-Rinke, K.; Kuhlbusch, T.; Van den Brink, N.; Nickel, C., Fate and
459   bioavailability of engineered nanoparticles in soils: a review. *Critical Reviews in Environmental*
460   *Science and Technology* **2014,** *44* (24), 2720-2764.
461   23.   Mozhayeva, D.; Engelhard, C. J. J. o. A. A. S., A critical review of single particle inductively
462   coupled plasma mass spectrometry–A step towards an ideal method for nanomaterial
463   characterization. **2020**.
464   24.   Hadioui, M.; Knapp, G. v.; Azimzada, A.; Jreije, I.; Frechette-Viens, L.; Wilkinson, K. J. J.
465   A. c., Lowering the size detection limits of Ag and TiO2 nanoparticles by Single Particle ICP-MS.
466   **2019,** *91* (20), 13275-13284.

467 25. Azimzada, A.; Farner, J. M.; Hadioui, M.; Liu-Kang, C.; Jreije, I.; Tufenkji, N.;
468 Wilkinson, K. J. J. E. S. N., Release of TiO2 nanoparticles from painted surfaces in cold climates:
469 characterization using a high sensitivity single-particle ICP-MS. **2020**.
470 26. Wigginton, N. S.; Haus, K. L.; Hochella Jr, M. F., Aquatic environmental nanoparticles.
471 *Journal of environmental monitoring* **2007,** *9* (12), 1306-1316.
472 27. del Real, A. E. P.; Castillo-Michel, H.; Kaegi, R.; Larue, C.; de Nolf, W.; Reyes-Herrera,
473 J.; Tucoulou, R.; Findling, N.; Salas-Colera, E.; Sarret, G. J. E. S. N., Searching for relevant criteria
474 to distinguish natural vs. anthropogenic TiO 2 nanoparticles in soils. **2018,** *5* (12), 2853-2863.
475 28. Von der Kammer, F.; Ferguson, P. L.; Holden, P. A.; Masion, A.; Rogers, K. R.; Klaine, S.
476 J.; Koelmans, A. A.; Horne, N.; Unrine, J. M., Analysis of engineered nanomaterials in complex
477 matrices (environment and biota): general considerations and conceptual case studies. *Environmental*
478 *Toxicology and Chemistry* **2012,** *31* (1), 32-49.
479 29. Azimzada, A.; Farner, J. M.; Jreije, I.; Hadioui, M.; Liu-Kang, C.; Tufenkji, N.; Shaw, P.;
480 Wilkinson, K. J., Single-and multi-element quantification and characterization of TiO2 nanoparticles
481 released from outdoor stains and paints. *Frontiers in Environmental Science* **2020**.
482 30. Janković, N. Z.; Plata, D. L., Engineered nanomaterials in the context of global element
483 cycles. *Environmental Science: Nano* **2019,** *6* (9), 2697-2711.
484 31. Pace, H. E.; Rogers, N. J.; Jarolimek, C.; Coleman, V. A.; Higgins, C. P.; Ranville, J. F. J.
485 A. c., Determining transport efficiency for the purpose of counting and sizing nanoparticles via single
486 particle inductively coupled plasma mass spectrometry. **2011,** *83* (24), 9361-9369.
487 32. Laborda, F.; Gimenez-Ingalaturre, A. C.; Bolea, E.; Castillo, J. R., Single particle
488 inductively coupled plasma mass spectrometry as screening tool for detection of particles.
489 *Spectrochimica Acta Part B: Atomic Spectroscopy* **2019,** *159*, 105654.
490 33. Shaw, P.; Donard, A., Nano-particle analysis using dwell times between 10 μs and 70 μs with
491 an upper counting limit of greater than 3×10 7 cps and a gold nanoparticle detection limit of less
492 than 10 nm diameter. *Journal of Analytical Atomic Spectrometry* **2016,** *31* (6), 1234-1242.
493 34. Groot Zwaaftink, C. D.; Arnalds, Ó.; Dagsson-Waldhauserova, P.; Eckhardt, S.; Prospero,
494 J. M.; Stohl, A., Temporal and spatial variability of Icelandic dust emissions and atmospheric
495 transport. *Atmospheric Chemistry and Physics* **2017,** *17* (17), 10865-10878.
496 35. Urupina, D.; Lasne, J.; Romanias, M.; Thiery, V.; Dagsson-Waldhauserova, P.; Thevenet,
497 F., Uptake and surface chemistry of SO2 on natural volcanic dusts. *Atmospheric Environment* **2019,**
498 *217*, 116942.
499 36. Gondikas, A.; Gallego-Urrea, J.; Halbach, M.; Derrien, N.; Hassellöv, M., Nanomaterial
500 fate in seawater: A rapid sink or intermittent stabilization? *Frontiers in Environmental Science* **2020,**
501 *8*, 151.
502 37. Labille, J.; Slomberg, D.; Catalano, R.; Robert, S.; Apers-Tremelo, M.-L.; Boudenne, J.-
503 L.; Manasfi, T.; Radakovitch, O., Assessing UV filter inputs into beach waters during recreational
504 activity: A field study of three French Mediterranean beaches from consumer survey to water
505 analysis. *Science of the Total Environment* **2020,** *706*, 136010.
506 38. Hao, Z.; Li, F.; Liu, R.; Zhou, X.; Mu, Y.; Sharma, V. K.; Liu, J.; Jiang, G., Reduction of
507 Ionic Silver by Sulfur Dioxide as a Source of Silver Nanoparticles in the Environment.
508 *Environmental Science & Technology* **2021**.
509 39. Wiklund, J. A.; Kirk, J. L.; Muir, D. C.; Gleason, A.; Carrier, J.; Yang, F., Atmospheric
510 trace metal deposition to remote Northwest Ontario, Canada: Anthropogenic fluxes and inventories
511 from 1860 to 2010. *Science of The Total Environment* **2020,** *749*, 142276.
512 40. Levard, C.; Hotze, E. M.; Lowry, G. V.; Brown Jr, G. E., Environmental transformations of
513 silver nanoparticles: impact on stability and toxicity. *Environmental science & technology* **2012,** *46*
514 (13), 6900-6914.

515 41. Wang, J.; Nabi, M. M.; Mohanty, S. K.; Afrooz, A. N.; Cantando, E.; Aich, N.; Baalousha,
516 M., Detection and quantification of engineered particles in urban runoff. *Chemosphere* **2020,** *248*,
517 126070.
518 42. Slomberg, D. L.; Auffan, M.; Guéniche, N.; Angeletti, B.; Campos, A.; Borschneck, D.;
519 Aguerre-Chariol, O.; Rose, J., Anthropogenic release and distribution of titanium dioxide particles in
520 a river downstream of a nanomaterial manufacturer industrial site. *Frontiers in Environmental*
521 *Science* **2020**.
522 43. Gondikas, A.; von der Kammer, F.; Kaegi, R.; Borovinskaya, O.; Neubauer, E.;
523 Navratilova, J.; Praetorius, A.; Cornelis, G.; Hofmann, T., Where is the nano? Analytical
524 approaches for the detection and quantification of TiO 2 engineered nanoparticles in surface waters.
525 *Environmental Science: Nano* **2018,** *5* (2), 313-326.
526 44. Rahim, M. F.; Pal, D.; Ariya, P. A., Physicochemical studies of aerosols at Montreal Trudeau
527 Airport: The importance of airborne nanoparticles containing metal contaminants. *Environmental*
528 *pollution* **2019,** *246*, 734-744.
529 45. Frisia, S.; Weyrich, L. S.; Hellstrom, J.; Borsato, A.; Golledge, N. R.; Anesio, A. M.;
530 Bajo, P.; Drysdale, R. N.; Augustinus, P. C.; Rivard, C., The influence of Antarctic subglacial
531 volcanism on the global iron cycle during the Last Glacial Maximum. *Nature communications* **2017,**
532 *8* (1), 1-9.
533 46. Heinlaan, M.; Ivask, A.; Blinova, I.; Dubourguier, H.-C.; Kahru, A., Toxicity of nanosized
534 and bulk ZnO, CuO and TiO2 to bacteria Vibrio fischeri and crustaceans Daphnia magna and
535 Thamnocephalus platyurus. *Chemosphere* **2008,** *71* (7), 1308-1316.
536 47. Aruoja, V.; Pokhrel, S.; Sihtmäe, M.; Mortimer, M.; Mädler, L.; Kahru, A., Toxicity of 12
537 metal-based nanoparticles to algae, bacteria and protozoa. *Environmental Science: Nano* **2015,** *2* (6),
538 630-644.
539 48. Wigger, H.; Kägi, R.; Wiesner, M.; Nowack, B., Exposure and Possible Risks of Engineered
540 Nanomaterials in the Environment—Current Knowledge and Directions for the Future. *Reviews of*
541 *Geophysics* **2020,** *58* (4), e2020RG000710.
542 49. Westerhoff, P.; Atkinson, A.; Fortner, J.; Wong, M. S.; Zimmerman, J.; Gardea-Torresdey,
543 J.; Ranville, J.; Herckes, P., Low risk posed by engineered and incidental nanoparticles in drinking
544 water. *Nature nanotechnology* **2018,** *13* (8), 661.
545 50. Yang, Y.; Chen, B.; Hower, J.; Schindler, M.; Winkler, C.; Brandt, J.; Di Giulio, R.; Ge,
546 J.; Liu, M.; Fu, Y., Discovery and ramifications of incidental Magnéli phase generation and release
547 from industrial coal-burning. *Nature communications* **2017,** *8* (1), 1-11.
548 51. Praetorius, A.; Gundlach-Graham, A.; Goldberg, E.; Fabienke, W.; Navratilova, J.;
549 Gondikas, A.; Kaegi, R.; Günther, D.; Hofmann, T.; von der Kammer, F., Single-particle multi-
550 element fingerprinting (spMEF) using inductively-coupled plasma time-of-flight mass spectrometry
551 (ICP-TOFMS) to identify engineered nanoparticles against the elevated natural background in soils.
552 *Environmental Science: Nano* **2017,** *4* (2), 307-314.
553 52. Yang, X.; Liu, X.; Zhang, A.; Lu, D.; Li, G.; Zhang, Q.; Liu, Q.; Jiang, G., Distinguishing
554 the sources of silica nanoparticles by dual isotopic fingerprinting and machine learning. *Nature*
555 *communications* **2019,** *10* (1), 1620.

556